

SU(2)_{CMB} at high redshifts and the value of H_0

Steffen Hahn¹, Ralf Hofmann²

¹Karlsruhe Institute of Technology, Laboratory for Applications of Synchrotron Radiation, Kaiserstr. 12, Karlsruhe D-76131, Germany

²Universität Heidelberg, Institut für Theoretische Physik, Philosophenweg 16, Heidelberg D-69120, Germany

Accepted XXX. Received YYY; in original form ZZZ

ABSTRACT

We investigate a high- z cosmological model to compute the co-moving sound horizon r_s at baryon-velocity freeze-out towards the end of hydrogen recombination. This model assumes a replacement of the conventional CMB photon gas by deconfining SU(2) Yang-Mills thermodynamics, three flavours of massless neutrinos ($N_\nu = 3$), and a purely baryonic matter sector (no cold dark-matter (CDM)). The according SU(2) temperature-redshift relation of the CMB is contrasted with recent measurements appealing to the thermal Sunyaev-Zel’dovich effect and CMB-photon absorption by molecular rotations bands or atomic hyperfine levels. Relying on a realistic simulation of the ionization history throughout recombination, we obtain $z_* = 1693.55 \pm 6.98$ and $z_{\text{drag}} = 1812.66 \pm 7.01$. Due to considerable widths of the visibility functions in the solutions to the associated Boltzmann hierarchy and Euler equation we conclude that z_* and z_{drag} over-estimate the redshifts for the respective photon and baryon-velocity freeze-out. Realistic decoupling values turn out to be $z_{\text{f},*} = 1554.89 \pm 5.18$ and $z_{\text{f,drag}} = 1659.30 \pm 5.48$. With $r_s(z_{\text{f,drag}}) = (137.19 \pm 0.45)$ Mpc and the essentially model independent extraction of $r_s \cdot H_0 = \text{const}$ from low- z data in arXiv:1607.05617 we obtain a good match with the value $H_0 = (73.24 \pm 1.74)$ km s⁻¹ Mpc⁻¹ extracted in arXiv:1604.01424 by appealing to Cepheid calibrated SNe Ia, new parallax measurements, stronger constraints on the Hubble flow, and a refined computation of distance to NGC4258 from maser data. We briefly comment on a possible interpolation of our high- z model, invoking percolated and unpercolated U(1) topological solitons of a Planck-scale axion field, to the phenomenologically successful low- z Λ CDM cosmology.

Key words: cosmic background radiation – cosmological parameters – dark matter – distance scale – cosmology: theory

1 INTRODUCTION

The last two and a half decades have witnessed a tremendous industry in collecting and interpreting precise observational data to determine the cosmology of our universe: (i) large-scale structure surveys confirming the existence of a standard ruler r_s set by the physics of baryonic acoustic oscillations throughout the epochs preceding and including the recombination of primordial helium and hydrogen, e.g. Abazajian et al. (2003); Adelman-McCarthy et al. (2008), (ii) observations of the cosmic microwave background (CMB), confirming its black-body nature and revealing the CMB decoupling physics as well as associated primordial statistical properties of matter and hence temperature fluctuations, e.g. Mather et al. (1990); Hinshaw et al. (2013); Ade et al. (2014a), and (iii) use of calibrated standard candles in luminosity distance-redshift observations, ultimately changing the paradigm on late-time expansion history (low- z regime) Perlmutter et al. (1998); Riess et al. (1998). As a consequence, we now appear to possess an accurate parametriza-

tion of the universe’s composition in terms of the standard Λ CDM concordance model. Yet, we suspect that this model is prone to over-simplification: So far there is no falsifiable theory on what the dark sector actually is made of. Moreover, as we shall argue in the present work, the extrapolation of the observationally well established low- z model to thermal expansion history well before and including CMB decoupling, although seemingly in accord with the results of Hinshaw et al. (2013); Ade et al. (2014a), can be misleading.

In Hofmann (2015) the implication of a new SU(2) Yang-Mills theory, describing the CMB as a gas of thermal photons supplemented by a thermal ground state and two invisible vector mode V^\pm , towards the temperature-redshift (T - z) relation was analysed within an Friedmann-Lemaître-Robertson-Walker (FLRW) universe. Due to non-conformal scaling at low z this relation suffers a lower linear slope at

arXiv:1611.02561v3 [physics.gen-ph] 29 Mar 2017

high z ($z \gtrsim 9$) compared to the standard U(1) theory¹,

$$\begin{aligned} \frac{T}{T_0} &= z + 1, \quad (\text{U}(1), \forall z) \quad \longrightarrow \\ \frac{T}{T_0} &= 0.63(z + 1), \quad (\text{SU}(2)_{\text{CMB}}, z \gtrsim 9), \end{aligned} \quad (1)$$

see also Fig. 1. We refrain here from reviewing the entire thermodynamics of an SU(2) Yang-Mills theory in its deconfining phase. We also skip a discussion of why the critical temperature $T_c = T_0$ ($T_0 = 2.725$ K referring to the present CMB temperature) for the onset of the deconfining-preconfining phase transition in such a theory is fixed by low-frequency observation of the present CMB, justifying the name SU(2)_{CMB}. To be informed about all this in a pragmatic way we refer the reader to Hofmann (2015), for an in-depth read we propose Hofmann (2016a). We do mention though that the standard relation between neutrino temperature T_ν and T , $T_\nu = (4/11)^{1/3} T$, obtained from entropy conservation during e^+e^- annihilation, modifies in SU(2)_{CMB} to

$$\frac{T_\nu}{T} = \left(\frac{g_1}{g_0} \right)^{1/3} = \left(\frac{16}{23} \right)^{1/3}. \quad (2)$$

This is because $g_0 = 8 + (7/8)4$ (number of relativistic degrees of freedom (d.o.f.) before annihilation) and $g_1 = 8$ (d.o.f. after annihilation), see Hofmann (2015). Note that for, say, $z > 100$ SU(2)_{CMB}'s two massive vector excitations V^\pm can be considered highly relativistic. Namely, for $z > 100$ one has $m_{V^\pm}/T < 1.4 \times 10^{-3}$ such that the energy density $\rho_{\text{SU}(2)_{\text{CMB}}}$ is due to eight relativistic d.o.f.

The SU(2)_{CMB} relation (1) and Fig. 1 represent a strong deviation from the conventional relation $\frac{T}{T_0} = z + 1$, the latter being a direct consequence of the conformal, thermal photon-gas equation of state $p_\gamma = \frac{1}{3}\rho_\gamma$. In SU(2)_{CMB}, however, this equation of state is non-conformal because it incorporates the thermal ground state as well as free vector-boson excitations whose mass derives from an adjoint Higgs mechanism, representing a tight coupling to the thermal ground state. As such, the entire deconfining thermodynamics of SU(2)_{CMB} is influenced by a fixed (Yang-Mills) mass scale $\Lambda_{\text{CMB}} \sim 10^{-4}$ eV Hofmann (2016a). However, the purely photonic part of SU(2)_{CMB} is still conformal², at least on the level of free thermal quasiparticle fluctuations which is sufficiently accurate for our purposes. Therefore and because of adiabatically slow cosmological expansion the gas of thermal photons solely is governed by (redshift dependent) temperature T . As a consequence, a quantity of dimension mass (natural units: $c = \hbar = k_B = 1$) describing the spectral

properties of the thermal photon gas, say, the circular frequency ω of a thermal photon, is expressible as a *redshift independent*, dimensionless multiple x of T ,

$$\omega = xT. \quad (3)$$

Literature testifies to proposed and actual measurements of the CMB temperature T as a function of redshift z by appealing to the thermal Sunyaev-Zel'dovich (tSZ) effect ($z \leq 1$). This effect represents small negative (low x) or positive (high x) shifts ΔI_{tSZ} of spectral intensity compared to the CMB black-body spectrum caused by (recoil-free) interaction of CMB photons with electrons in high-temperature plasmas ($T_e \sim 10$ keV) occurring in galaxy clusters, see, e.g. Rephaeli (1980); Luzzi et al. (2015). Other extractions of $T(z)$ appeal to the excitation of molecular rotation bands or atomic hyperfine lines by interaction with the CMB, see, e.g. Muller et al. (2013). For the tSZ effect one has

$$\Delta I_{\text{tSZ}} = \frac{T_0^3}{2\pi^2} \frac{x^4 e^x}{(e^x - 1)^2} \tau (\theta f(x) - v_r + C(x, \theta, v_r)), \quad (4)$$

where $\tau = \sigma_T \int dl n_e$ is the optical depth (σ_T the Thomson-scattering cross section; $\int dl n_e$ the electron density, projected through the cluster along the line of sight), $\theta \equiv \frac{T_e}{m_e}$ (m_e rest mass of electron), v_r denotes the radial component of the cluster's peculiar velocity, and $f(x) \equiv x \coth \frac{x}{2} - 4$. Function C describes (small) relativistic corrections. ΔI_{tSZ} can be conceived as the linear term in a spectrally local temperature shift

$$\Delta T_{\text{tSZ}} \equiv T_0 \tau (\theta f(x) - v_r + C(x, \theta, v_r)) \quad (5)$$

when expanding spectral intensity about the undistorted black-body spectrum: The factor $\frac{T_0^3}{2\pi^2} \frac{x^4 e^x}{(e^x - 1)^2}$ represents the first derivative of black-body spectral intensity w.r.t. temperature T at $T = T_0$. Notice that ΔI_{tSZ} depends on the CMB photon circular frequency ω through the dimensionless variable x only whose z -independence is a consequence of the one-scale (or conformal) nature of the undistorted thermal photon gas as discussed above. Furthermore, there are dependences on dimensionless quantities, θ and v_r . However, statistically seen, θ and v_r are not expected to be z -dependent. ΔI_{tSZ} thus is redshift independent to linear order in ΔT_{tSZ} . Organizing the tSZ effect as an expansion in powers of ΔT_{tSZ} , the dependence on ω of the coefficients of higher-than-linear powers in ΔT_{tSZ} may no longer occur solely via x . This would violate the exact z -independence of ΔI_{tSZ} at an immeasurable level, however. Based on these observations it is clear that the tSZ effect cannot be used to extract $T(z)$: The usual prejudice that the circular frequency ω of a thermal CMB photon is blueshifted as $\omega = (z + 1)\omega_0$ Luzzi et al. (2015) immediately implies that also $T = (z + 1)T_0$. This, indeed, is "extracted" from the data. Conversely, the theoretical prediction of $T(z) = g(z)T_0$ (g the dimensionless function encoded in Fig. 1), being a consequence of SU(2)_{CMB} energy conservation in a FLWR universe Hofmann (2015), immediately implies the according blueshift law $\omega = g(z)\omega_0$ for the circular frequency of a CMB photon. Since CMB photons in contrast to propagating electromagnetic waves are *incoherent* fluctuations such a blueshift law has no exploitable information content. In this context we stress that the observation of redshifts of frequencies in atomic emission spectra

¹ In Eq. (1) a slight and inessential correction of the high- z coefficient from 0.62 in Hofmann (2015) to 0.63 is performed which is due to a more precise initial-condition matching for the solution to the energy-conservation equation.

² The way how the SU(2)_{CMB} photon gas relates to its thermal ground state respects this disconnectness from scale Λ_{CMB} microscopically: Energy and momentum quanta are invoked by inert (anti)caloron centers, which themselves are energy and momentum free, while a small low-frequency spectral range of wavelike excitations only appeals to polarisable electric and magnetic dipole densities whose dipole moments and associated volume per dipole moment, again, are determined by inert (anti)caloron centers, see Hofmann (2016b).

from astrophysical objects are a completely nonthermal affair: These spectra are propagated towards the observer by directed, *wave-like* disturbances subject to the U(1) Cartan subgroup of an SU(2) gauge group subject to a Yang-Mills scale largely disparate from $\Lambda_{\text{CMB}} \sim 10^{-4}$ eV Hofmann (2016b). Recall, that the blueshift $\nu = (z+1)\nu_0$ of observed frequency ν_0 is an immediate consequence of the emitted wave traveling along a null-geodesic in FLRW cosmology. As for the "extraction" of $T(z)$ in terms of the temperature setting the thermally weighted population of hyperfine atomic or rotational molecular levels upon radiative coupling of the considered species with the CMB, one also assumes that a CMB photon frequency ν , which matches a transition frequency, is redshifted according to the conventional theory, see, e.g. Muller et al. (2013). However, since the frequency dependence of the associated column density rests on Boltzmann exponentials of CMB temperature T , this prejudice prescribes $T(z)$ in the sense discussed above: $T(z)$ necessarily is "extracted" to be conventional. As an aside, we point out in Appendix B, Fig. B1, that the usual power-law parametrisation $T(z) = (1+z)^{1-\beta}T_0$ (β fixed) in observational "extractions" of $T(z)$ is not satisfactory when confronted with the low- z behaviour of $T(z)$ shown in Fig. 1.

Because of relation (1) CMB decoupling sets in at a redshift of ~ 1800 which is highly disparate from $z \sim 1100$ purported by the Λ CDM concordance model. As discussed in Hofmann (2015), this suggests that at CMB decoupling the role of non-relativistic matter in Λ CDM cosmology, composed of cold dark and baryonic contributions, is played solely by the baryons. The question then arises how the well-tested Λ CDM model emerges at intermediate redshifts. Based on percolated and unpercolated solitons Wetterich (2001) of a Planck-scale axion field (U(1) vortices) Appendix D proposes a possible answer. To clarify whether such a scenario can explain the observed rotation curves of spiral galaxies and the extensive data on structure formation – thus seeded by Planckian physics and phase transitions in the early universe – *much more* work is required.

The present paper therefore adopts the point of view that for cosmological purposes the Λ CDM model is a useful and accurate approximation to the actual physics for $z \lesssim 9$. At the same time, we suspect that for higher values of z this model increasingly fails because of relation (1). Fortunately, our high- z cosmological model, which is conservative concerning its (solely baryonic) matter content and the number of massless neutrino flavours but invokes $SU(2)_{\text{CMB}}$ to describe the CMB itself, can be tested in terms of the most basic low- z cosmological parameter: today's value of the cosmic expansion rate H_0 . This test relies on an inverse proportionality between the co-moving sound horizon at baryon freeze-out r_s and H_0 which was extracted from low- z data (Cepheid calibrated SNe Ia, new parallax measurements, stronger constraints on the Hubble flow, and a refined computation of distance to NGC4258 from maser data) under no model assumptions other than spatial flatness, SNe Ia/ r_s yielding standard candles/a standard ruler, and a smooth expansion history Bernal, Verde & Riess (2016). Obviously, this knowledge is important because it allows a high- z extraction of r_s to determine H_0 . Note that the value of H_0 , as obtained by CMB analysis based on Λ CDM and U(1) photons Ade et al. (2016), is at 3.4σ tension with the direct measurement of H_0 in Riess et al. (2016).

When (re-)computing r_s in the new, high- z $SU(2)_{\text{CMB}}$ based model with $N_\nu = 3$ massless neutrinos, $T_0 = 2.725$ K, and solely baryonic matter (simply referred to $SU(2)_{\text{CMB}}$ in the following) and in the Λ CDM model we consider the parameter values of $\eta_{10}, Y_P, N_{\text{eff}}$, and Ω_{CDM} of Ade et al. (2016) as representative, see Sec. 2.

This work is organized as follows. In Sec. 2 we introduce $SU(2)_{\text{CMB}}$ and discuss its parameter setting. A rough estimate of the decoupling redshift z_{dec} , obtained by assuming (i) thermalization (Saha equation) and (ii) instantaneous decoupling, is carried out for both $SU(2)_{\text{CMB}}$ and Λ CDM in Sec. 3. Comparing our value for z_{dec} with the values for z_* and z_{drag} in Λ CDM, we conclude that this approximation systematically over-estimates the conventional redshift values for decoupling and baryon velocity freeze-out. This led us to perform a realistic simulation of the recombination physics in Sec. 4 based on the Boltzmann code **recfast**, the simulation for Λ CDM serving as a check in reproducing the values for $r_s(z_{\text{drag}})$ and $r_s(z_*)$ of Ade et al. (2016). For $SU(2)_{\text{CMB}}$ we find that $z_{\text{drag}} > z_*$. Because the visibility functions in the formal solutions of the Boltzmann hierarchy for the temperature perturbations and of the Euler equation for baryon velocity are not delta-like, as assumed in Hu & Sugiyama (1996), but exhibit considerable widths freeze-out redshifts $r_s(z_{\text{lf,drag}})$ and $r_s(z_{\text{lf,*}})$ are determined by the left flanks of these visibility functions rather than their centers. Subsequently, we compute $r_s(z_{\text{lf,*}})$ and $r_s(z_{\text{lf,drag}})$. With the $r_s - H_0$ relation of Bernal, Verde & Riess (2016) we deduce from our value of $r_s(z_{\text{lf,drag}})$ a good match of H_0 with the value given in Riess et al. (2016). In Sec. 5 we summarize our results, briefly discuss a cosmological model, which, based on topological solitons of a Planck-scale axion field, interpolates our high- z $SU(2)_{\text{CMB}}$ model with low- z Λ CDM, and sketch a road map for future work. Appendix A contains a table documenting the changes in the **recfast** code when adapted to $SU(2)_{\text{CMB}}$. Appendix B addresses peculiarities in fitting $T(z)$ for $SU(2)_{\text{CMB}}$. Appendix C investigates the solution to the Euler equation describing baryon-velocity evolution to argue that freeze-out occurs at $z_{\text{lf,drag}}$ rather than z_{drag} . Appendix D provides technical details on a high- z to low- z interpolating cosmological model together with a computation of the angular scale θ_* associated with the sound horizon at photon freeze-out which is observable in the CMB TT correlation function.

2 HIGH-Z COSMOLOGICAL MODEL AND SOUND HORIZON

Let us introduce our high- z cosmological model $SU(2)_{\text{CMB}}$. As usual, a subscript "0" refers to today's value of the associated quantity, we work in super-natural units ($c = \hbar = k_B = 1$), and we assume a spatially flat FLRW universe such that

$$H(z) = H_0 \sqrt{\sum_i \Omega_i(z)}, \quad (6)$$

with $\Omega_i(z=0) \equiv \Omega_{i,0}$ defining the ratio of today's energy density $\rho_{i,0}$ of the i th separately conserved (and at $z \gg 1$ relevant) cosmic fluid to today's critical density $\rho_{c,0} \equiv 3/(8\pi G)H_0^2$. Here G denotes Newton's constant. Fur-

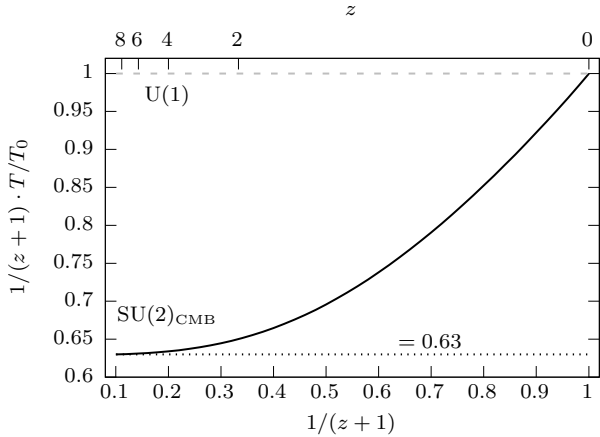


Figure 1. The T - z scaling relation $T/(T_0(z+1))$ in $SU(2)_{\text{CMB}}$ (solid). Note the emergence of $T/T_0 = 0.63(z+1)$ for $z \gtrsim 9$ (dotted). The conventional $U(1)$ theory for thermal photon gases associates with the dashed line. Data taken from Hofmann (2015) after slight and inessential correction.

thermore, we make the convention

$$H_0 \equiv h 100 \text{ km s}^{-1} \text{ Mpc}^{-1}. \quad (7)$$

We consider $N_\nu = 3$ flavours of massless neutrinos Beringer et al. (2012) to form a separately conserved cosmic fluid. Because of $SU(2)_{\text{CMB}}$ the neutrino temperature T_ν is determined by the CMB temperature T as in Eq. (2), and their energy density ρ_ν relates to the energy density of CMB photons ρ_γ as

$$\rho_\nu(T) = \frac{7}{8} \left(\frac{16}{23} \right)^{4/3} N_\nu \rho_\gamma(T). \quad (8)$$

Because eight instead of two relativistic d.o.f. determine the energy density $\rho_{SU(2)_{\text{CMB}}}$ at high- z one has

$$\rho_{SU(2)_{\text{CMB}}}(T) = 4 \rho_\gamma(T). \quad (9)$$

Writing $\rho_{SU(2)_{\text{CMB}}}$ as a function of z , Eq. (1) implies

$$\rho_{SU(2)_{\text{CMB}}}(z) = A \rho_{\gamma,0}(z+1)^4, \quad (10)$$

where

$$A \equiv (8/2) \cdot (0.63)^4. \quad (11)$$

Considering Eq. (6), Eqs. (10) and (8) are recast as

$$\rho_{SU(2)_{\text{CMB}}}(z) = A H_0^2 \Omega_{\gamma,0}(z+1)^4 \frac{3}{8\pi G}, \quad (12)$$

and

$$\rho_\nu(z) = \frac{7}{8} \frac{A}{4} \left(\frac{16}{23} \right)^{4/3} N_\nu H_0^2 \Omega_{\gamma,0}(z+1)^4 \frac{3}{8\pi G}. \quad (13)$$

Setting $T_0 = 2.725 \text{ K}$ Fixsen et al. (1996), one has $\Omega_{\gamma,0} = 2.46796 \times 10^{-5} h^{-2}$.

Non-relativistic, cosmological matter is assumed to be purely baryonic in $SU(2)_{\text{CMB}}$. Its energy density today, $\rho_{b,0}$, relates to $\rho_{\gamma,0}$ as

$$\rho_{b,0} = \frac{4}{3} R_0 \rho_{\gamma,0} \quad (14)$$

such that

$$R_0 \equiv 111.019 \eta_{10}, \quad (15)$$

where

$$R \equiv \frac{3}{4} \frac{\rho_b}{\rho_\gamma}. \quad (16)$$

From Big-Bang Nucleosynthesis (BBN) η_{10} is constrained to $4.931 \leq \eta_{10} \leq 7.123$, see Fig. 29 in Ade et al. (2014b). The number η_{10} parametrises today's baryon-to-photon number-density ratio $n_{b,0}/n_{\gamma,0}$ as

$$n_{b,0}/n_{\gamma,0} \equiv \eta_{10} \times 10^{-10}. \quad (17)$$

Note that the central value in

$$\eta_{10} = 6.08232 \pm 0.06296, \quad (18)$$

as computed from the value $\Omega_{b,0} = (0.02222 \pm 0.00023) h^{-2}$ obtained by the Planck collaboration Ade et al. (2016), is also central to the above BBN range. According to Ade et al. (2016) this value of η_{10} implies a ${}^4\text{He}$ mass fraction Y_P of

$$Y_P = 0.252 \pm 0.041. \quad (19)$$

Note that due to non-conformal T - z scaling in $SU(2)_{\text{CMB}}$ there is a low- z dependence of n_b/n_γ – in contrast to the conventional case of $U(1)$ photons. Also, because of Eq. (1) the high- z expression for quantity R reads

$$R(z) \equiv 111.019 \frac{\eta_{10}}{(0.63)^4(z+1)}. \quad (20)$$

Taking the central value for η_{10} from Eq. (18), appealing to $T_{\text{dec}} \sim 3000 \text{ K}$, and considering Eq. (1), we roughly estimate the redshift z_{dec} for the end of hydrogen recombination as $z_{\text{dec}} \sim 3000/(0.63 \cdot 2.725) - 1 \sim 1775$. Therefore, we conclude from Eq. (15) that in $SU(2)_{\text{CMB}}$ $R(z) > 1$ for z ranging from $z = 0$ to well beyond recombination: $R(z) > 1$ for $z < 4568$. This is in contrast to the conventional ΛCDM model where CMB decoupling occurs at $z_{\text{dec}} \sim 1100$ and where R is given as

$$R(z) \equiv 111.019 \frac{\eta_{10}}{z+1} \quad (21)$$

such that $R(z) < 1$ for $z > 675$. As usual we have

$$\frac{\rho_b(z)}{\rho_{c,0}} \equiv \Omega_{b,0}(z+1)^3, \quad (22)$$

where Ade et al. (2016)

$$\Omega_{b,0} \equiv 0.00365321 \eta_{10} h^{-2}. \quad (23)$$

Therefore, in $SU(2)_{\text{CMB}}$ the high- z Hubble parameter H reads

$$H(z) = H_0 \left[\Omega_{b,0}(z+1)^3 + A \left(1 + \frac{7}{32} \left(\frac{16}{23} \right)^{4/3} N_\nu \right) \Omega_{\gamma,0}(z+1)^4 \right]^{1/2}, \quad (24)$$

where $\Omega_{b,0}$ and its errors derive from η_{10} as quoted in Eq. (18). We also consider the high- z ΛCDM model

$$H(z) = H_0 \left[(\Omega_{b,0} + \Omega_{\text{CDM}})(z+1)^3 + \left(1 + \frac{7}{8} \left(\frac{4}{11} \right)^{4/3} N_{\text{eff}} \right) \Omega_{\gamma,0}(z+1)^4 \right]^{1/2}, \quad (25)$$

Table 1. Cosmological high- z models: Λ CDM versus $SU(2)_{\text{CMB}}$.

	Λ CDM	$SU(2)_{\text{CMB}}$
$\frac{T}{T_0}$	$z + 1$	$0.63(z + 1)$
$\frac{T_L}{T}$	$\left(\frac{4}{11}\right)^{1/3}$	$\left(\frac{16}{23}\right)^{1/3}$
Ω_{CDM}	Ω_{CDM}	0
N_ν	N_{eff}	3

where according to Ade et al. (2016) we have

$$\Omega_{\text{CDM}} = (0.1197 \pm 0.0022) h^{-2}, \quad N_{\text{eff}} = 3.15 \pm 0.23. \quad (26)$$

Note that in both cases, Eqs. (24) and (25), the high- z expressions for $H(z)$ are independent of h . An overview of the differences between high- z Λ CDM and $SU(2)_{\text{CMB}}$ is presented in Tab. 1.

The co-moving sound horizon $r_s(z)$, as emergent within the baryon-electron-photon plasma, is defined as

$$r_s(z) = \int_0^{\eta(z)} d\eta' c_s(\eta') = \int_z^\infty dz' \frac{c_s(z')}{H(z')}, \quad (27)$$

where η is conformal time ($d\eta \equiv dt/a$), and c_s denotes the sound velocity, given as

$$c_s \equiv \frac{1}{\sqrt{3(1+R)}}. \quad (28)$$

In Eq. (28) R either needs to be taken from Eq. (20) ($SU(2)_{\text{CMB}}$) or from Eq. (21) (Λ CDM).

Finally, we would like to explain how we perform error estimates for $r_s(z)$. For example, in $SU(2)_{\text{CMB}}$ error-prone input parameters are η_{10} and Y_P . For those we generate pairs of Gaussian distributed random values. For each pair we compute $r_s(z)$ and fit a Gaussian to the ensuing histogram in order to extract the $1\text{-}\sigma$ error range for $r_s(z)$. In doing this, z needs to satisfy a condition, specified, e.g. by either Eqs. (38), (41), or (43), to determine its value z_{dec} , z_* , and z_{drag} , respectively. For Λ CDM the set $\{\eta_{10}, Y_P\}$ is enhanced by the elements Ω_{CDM} and N_{eff} . For an overview of the values of the cosmological parameters see Tab. 2.

3 SAHA EQUATION AND INSTANTANEOUS CMB DECOUPLING/RADIATION DRAG

Before we turn to a detailed analysis of recombination physics in Sec. 4, let us now perform a rough estimate for a single redshift z_{dec} associated with CMB decoupling physics/radiation drag (baryon velocity freeze-out). In the present section, we base our estimate on two assumptions: (i) thermalization (Saha equation) and (ii) coincidence of decoupling and radiation drag, both of vanishing duration.

Appealing to the results of Bernal, Verde & Riess (2016) on the low- z inverse proportionality between the sound horizon r_s , seen in today's baryonic matter correlation, and H_0 , our here-determined central value of H_0 for Λ CDM overestimates the result

$$H_0 = (67.31 \pm 0.96) \text{ km s}^{-1} \text{ Mpc}^{-1} \quad (29)$$

of Ade et al. (2016). Also, our estimate of H_0 for $SU(2)_{\text{CMB}}$

is higher than the directly measured value

$$H_0 = (73.24 \pm 1.74) \text{ km s}^{-1} \text{ Mpc}^{-1} \quad (30)$$

of Riess et al. (2016). This motivates our analysis of Sec. 4.

In the present section, the value of z_{dec} is determined from condition

$$H(z_{\text{dec}}) = \Gamma(z_{\text{dec}}). \quad (31)$$

In Eq. (31) the rate Γ for scattering of eV-photons off free, non-relativistic electrons reads

$$\Gamma = \sigma_T n_e^b \chi_e, \quad (32)$$

where $\sigma_T \equiv 6.65 \times 10^{-25} \text{ cm}^2$ denotes the Thomson cross section for electron-photon scattering, and n_e^b is the electron density just before the onset of hydrogen recombination which is given as

$$\begin{aligned} n_e^b(z) &\equiv (1 - Y_P) n_b(z) \\ &= 410.48 \cdot 10^{-10} \eta_{10} (1 - Y_P) (z + 1)^3 \text{ cm}^{-3}. \end{aligned} \quad (33)$$

Moreover, χ_e refers to the ionization fraction during the recombination epoch,

$$\chi_e(z) \equiv \frac{n_e(z)}{n_e^b(z)}, \quad (34)$$

n_e being the actual electron density, evolving non-trivially during recombination, see Sec. 4. In our present treatment we set $z = z_{\text{dec}}$ in Eqs. (33) and (34). We also use the Saha equation, which assumes thermal equilibrium between electrons, photons, and ions,³

$$\frac{\chi_e^2}{1 - \chi_e} = \frac{1}{n_e^b} \left(\frac{T_{\text{dec}} m_e}{2\pi} \right)^{3/2} \exp\left(-\frac{B_H}{T_{\text{dec}}}\right) \equiv S, \quad (35)$$

to estimate χ_e^2 at z_{dec} . In Eq. (35) the following values are set for the quantities m_e, B_H :

$$m_e = 510998.94 \text{ eV}, \quad B_H = 13.6 \text{ eV}. \quad (36)$$

Depending on whether the cosmological model of Eq. (24) ($SU(2)_{\text{CMB}}$) or Eq. (25) (Λ CDM) is considered, we set in Eq. (35) $T_{\text{dec}} = 0.63(z_{\text{dec}} + 1)T_0$ or $T_{\text{dec}} = (z_{\text{dec}} + 1)T_0$, respectively. Solving Eq. (35) for χ_e , we have

$$\chi_e = \frac{1}{2} \left[-S + S^{1/2}(4 + S)^{1/2} \right] \sim S^{1/2} \quad (S \ll 1). \quad (37)$$

On the other hand, solving Eq. (31) for χ_e yields

$$\chi_e(z_{\text{dec}}) = \frac{1}{\sigma_T n_e^b(z_{\text{dec}})} H(z_{\text{dec}}), \quad (38)$$

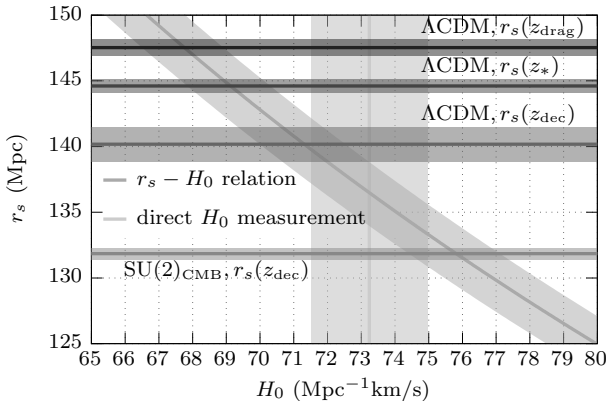
where either the expression in Eq. (24) ($SU(2)_{\text{CMB}}$) or in Eq. (25) (Λ CDM) is substituted for H . Equating the right-hand sides of Eq. (37) and Eq. (38) as foreseen by Eq. (31), we derive approximate values for z_{dec} and their errors from $\eta_{10}, Y_P, \Omega_{\text{CDM}}$, and N_{eff} as quoted in Eqs. (18), (19), and (26), respectively, see also Tab. 2. We obtain

$$\begin{aligned} z_{\text{dec}} &= 1760.14 \pm 1.85 \quad (SU(2)_{\text{CMB}}), \\ z_{\text{dec}} &= 1132.78 \pm 1.27 \quad (\Lambda\text{CDM}). \end{aligned} \quad (39)$$

³ Thomson scattering off neutral hydrogen and Helium atoms can safely be neglected Mukhanov (2005).

Table 2. Cosmological parameter values employed in the computations and their sources.

parameter	value	source
H_0 (SU(2) _{CMB})	$(73.24 \pm 1.74) \text{ km s}^{-1} \text{ Mpc}^{-1}$	Riess et al. (2016)
H_0 (Λ CDM)	$(67.31 \pm 0.96) \text{ km s}^{-1} \text{ Mpc}^{-1}$	TT+lowP, Ade et al. (2016)
T_0	2.725 K	Fixsen et al. (1996)
$\Omega_{\gamma,0}h^2$	2.46796×10^{-5}	based on $T_0 = 2.725$ K
$\Omega_{b,0}h^2$	0.02222 ± 0.99923	TT+lowP, Ade et al. (2016)
$\Omega_{\text{CDM},0}h^2$	0.1197 \pm 0.0022	TT+lowP, Ade et al. (2016)
η_{10}	6.08232 ± 0.06296	based on $\Omega_{\gamma,0}h^2$, TT+lowP, Ade et al. (2016)
Y_{P}	0.252 ± 0.041	TT, Ade et al. (2016)
N_{eff}	3.15 ± 0.23	abstract, Ade et al. (2016)

**Figure 2.** Instantaneous-decoupling predictions of the sound horizon r_s including the $1\text{-}\sigma$ error range in high- z Λ CDM (third horizontal band) and SU(2)_{CMB} (fourth horizontal band) together with the low- z r_s - H_0 relation of Bernal, Verde & Riess (2016) (curved band) and the direct measurement of H_0 as reported in Riess et al. (2016) (vertical band). For completeness we also quote $r_s(z_{\text{drag}})$ (first horizontal band) and $r_s(z_*)$ (second horizontal band) in Λ CDM, for definitions see Sec. 4.

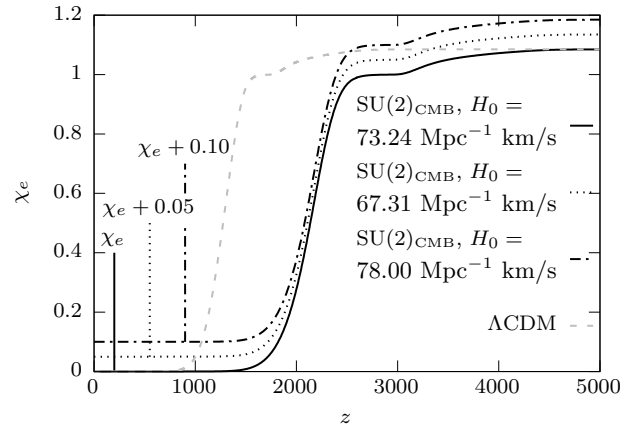
Appealing to Eq. (27), we arrive at

$$\begin{aligned} r_s(z_{\text{dec}}) &= (131.85 \pm 0.43) \text{ Mpc} \quad (\text{SU}(2)_{\text{CMB}}), \\ r_s(z_{\text{dec}}) &= (140.18 \pm 1.30) \text{ Mpc} \quad (\Lambda\text{CDM}), \end{aligned} \quad (40)$$

see Fig. 2. Amusingly, the intersections of the bands $r_s(z_{\text{dec}})$ in SU(2)_{CMB} and Λ CDM with the $r_s - H_0$ band of Bernal, Verde & Riess (2016) have a non-vanishing intersection with the $1\text{-}\sigma$ range of H_0 measured in Riess et al. (2016). However, we observe that $r_s(z_{\text{dec}})$ is considerably underestimated compared to $r_s(z_{\text{drag}})$ in Λ CDM. Therefore, we suspect that $r_s(z_{\text{dec}})$ is also underestimated in SU(2)_{CMB} compared to its true value at baryon freeze-out. Indeed, since $\chi_e(z_{\text{dec}}) = 0.003$ (SU(2)_{CMB}) and $\chi_e(z_{\text{dec}}) = 0.010$ (Λ CDM) we are left with considerable doubt on whether our present treatment yields reliable results.

4 REALISTIC TREATMENT OF RECOMBINATION

Here we would like to subject recombination physics to realistic histories of the ionization fraction $\chi_e(z)$. We appeal

**Figure 3.** Histories for the ionization fraction $\chi_e(z)$ in SU(2)_{CMB} (black with artificially introduced vertical offsets to distinguish curves for different values of H_0) and Λ CDM (gray, dashed) subject to the parameter values defined in Tab. 2, see also Sec. 2. Regions, for which $\chi_e(z) > 1$, associate with incomplete Helium recombination.

to the publically available Boltzmann code **recfast** Seager, Sasselov & Scott (1999, 2000); Wong, Moss & Scott (2008); Scott & Moss (2009) which also was used in Ade et al. (2014b). When computing $\chi_e(z)$ in SU(2)_{CMB} the following code adjustments need to be performed: re-set fnu from $\text{fnu}=21/8 \times (4/11)^{4/3}$ to $\text{fnu}=21/8 \times (23/16)^{4/3}$ ($N_{\text{eff}} = 3 = N_{\nu}$ by default) and re-define ranges in z for treatments by Saha, Peebles, or Boltzmann equation through divisions by 0.63. Note that for a fixed value of $\Omega_{b,0}$ (and $\Omega_{\text{CDM}} = 0$) the value H_0 can be varied in association with value of Ω_{Λ} such that the curvature term in $H(z)$ is nil. For an exposition of important changes when going from Λ CDM to SU(2)_{CMB}, see Tab. A1 in Appendix A. Our results for $\chi_e(z)$ do not depend on H_0 within a reasonable range, see Fig. 3.

The end of recombination at z_* is usually defined by the optical depth $\tau(z_*)$ to Thomson scattering from $z = 0$ to z_* being equal to unity Ade et al. (2014b). That is,

$$\tau(z_*) = \sigma_T \int_0^{z_*} dz \frac{\chi_e(z) n_e^b(z)}{(z+1)H(z)} = 1, \quad (41)$$

where $n_e^b(z)$ and $\chi_e(z)$ are defined in Eq. (33) and Eq. (34), respectively, and $H(z)$ either is given by Eq. (24) (SU(2)_{CMB}) or by Eq. (25) (Λ CDM). Due to a considerable

width of a bump-like weight function D_* (here referred to as visibility function) in the formal solution of the according Boltzmann hierarchy this criterion⁴ is revised in Appendix C. As a consequence, the position $z_{\text{lf},*}$ of the left flank of D_* is more realistic for photon decoupling.

We also consider the standard definition for the end of the radiation-drag epoch [Hu & Sugiyama \(1996\)](#), relying on the radiation-drag depth $\tau_{\text{drag}}(z)$, defined as

$$\tau_{\text{drag}}(z) = \sigma_T \int_0^z dz' \frac{\chi_e(z') n_e^b(z')}{(z'+1)H(z')R(z')}. \quad (42)$$

In [Hu & Sugiyama \(1996\)](#) the condition for freeze-out of baryonic velocity at z_{drag} is pronounced to be

$$\tau_{\text{drag}}(z_{\text{drag}}) = 1. \quad (43)$$

On the basis of the according Euler equation for the baryon-photon fluid we show in Appendix C, however, that the baryon velocity v_b is not yet frozen out at z_{drag} . Roughly speaking, the solution av_b of the Euler equation amounts to an z' -integral of D_{drag} (drag visibility function) resembling a bump-like function of *finite* width. Notice that D_{drag} was characterised as a delta function in [Hu & Sugiyama \(1996\)](#). Freeze-out, that is, z -independence of this integral, z being the lower integration limit, occurs if z is placed sufficiently far to the left of the position $z_{\text{max,drag}}$ of the maximum. A characteristic point $z_{\text{lf,drag}}$ setting a realistic cutoff for the z' -integration is the position of the left flank defined through the position of the maximum of the z' -derivative of D_{drag} . Interestingly, z_{drag} of Eq. (43) and $z_{\text{max,drag}}$ practically coincide. This would support the definition of baryon velocity freeze-out in Eq. (43) as in [Hu & Sugiyama \(1996\)](#) were it not for the finite width of D_{drag} . It is this finite width, however, which implies a substantial decrease from z_{drag} to $z_{\text{lf,drag}}$ in the redshift for baryon-velocity decoupling, see Appendix C for the technical argument and further discussions.

Using the parameter values of Sec. 2 and appealing to Eqs. (41), (27), and Fig. C2 in Appendix C, we obtain

$$\begin{aligned} z_* &= 1693.55 \pm 6.98 & (\text{SU}(2)_{\text{CMB}}), \\ z_{\text{lf},*} &= 1554.89 \pm 5.18 & (\text{SU}(2)_{\text{CMB}}), \\ z_* &= 1090.09 \pm 0.42 & (\Lambda\text{CDM}), \\ z_{\text{lf},*} &= 987.98 \pm 3.28 & (\Lambda\text{CDM}), \end{aligned} \quad (44)$$

and

$$\begin{aligned} r_s(z_*) &= (135.35 \pm 0.52) \text{ Mpc} & (\text{SU}(2)_{\text{CMB}}), \\ r_s(z_{\text{lf},*}) &= (143.34 \pm 0.42) \text{ Mpc} & (\text{SU}(2)_{\text{CMB}}), \\ r_s(z_*) &= (144.61 \pm 0.49) \text{ Mpc} & (\Lambda\text{CDM}), \\ r_s(z_{\text{lf},*}) &= (153.05 \pm 3.35) \text{ Mpc} & (\Lambda\text{CDM}). \end{aligned} \quad (45)$$

On the other hand, Eqs. (42), (27), and Fig. C1 in Appendix C yield

$$\begin{aligned} z_{\text{drag}} &= 1812.66 \pm 7.01 & (\text{SU}(2)_{\text{CMB}}), \\ z_{\text{lf,drag}} &= 1659.30 \pm 5.48 & (\text{SU}(2)_{\text{CMB}}), \\ z_{\text{drag}} &= 1059.57 \pm 0.46 & (\Lambda\text{CDM}), \\ z_{\text{lf,drag}} &= 973.12 \pm 3.06 & (\Lambda\text{CDM}), \end{aligned} \quad (46)$$

⁴ If D_* had a vanishing width then criterion (41) would be applicable.

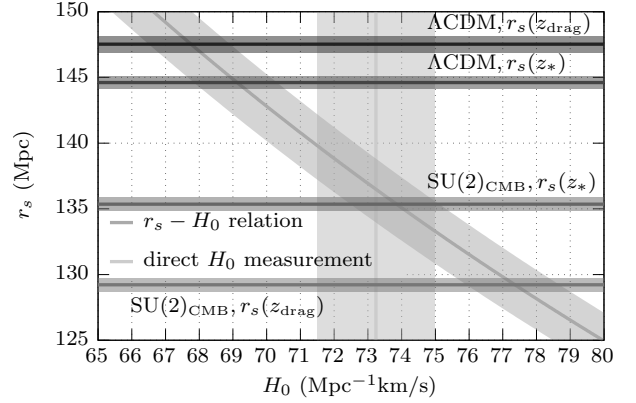


Figure 4. Predictions of the sound horizon r_s including the $1-\sigma$ error at z_* (second and third horizontal bands) and z_{drag} (first and fourth horizontal bands) in high- z ΛCDM and $\text{SU}(2)_{\text{CMB}}$, respectively. Also shown are the low- z r_s - H_0 relation of [Bernal, Verde & Riess \(2016\)](#) (curved band) and the direct measurement of H_0 (vertical band) as reported in [Riess et al. \(2016\)](#).

and

$$\begin{aligned} r_s(z_{\text{drag}}) &= (129.22 \pm 0.52) \text{ Mpc} & (\text{SU}(2)_{\text{CMB}}), \\ r_s(z_{\text{lf,drag}}) &= (137.19 \pm 0.45) \text{ Mpc} & (\text{SU}(2)_{\text{CMB}}), \\ r_s(z_{\text{drag}}) &= (147.33 \pm 0.49) \text{ Mpc} & (\Lambda\text{CDM}), \\ r_s(z_{\text{lf,drag}}) &= (154.57 \pm 3.33) \text{ Mpc} & (\Lambda\text{CDM}). \end{aligned} \quad (47)$$

For $\text{SU}(2)_{\text{CMB}}$ we have (central values of $z_{\text{lf},*}$ and $z_{\text{lf,drag}}$ only)

$$\chi_e(z_{\text{lf},*}) \sim 0.013, \quad \chi_e(z_{\text{lf,drag}}) \sim 0.032. \quad (48)$$

Fig. 4 indicates that, while the intersection of the $\text{SU}(2)_{\text{CMB}}$ -band for $r_s(z_{\text{drag}})$ with the $r_s - H_0$ band of [Bernal, Verde & Riess \(2016\)](#) is off the $1-\sigma$ range of the directly measured value of H_0 [Riess et al. \(2016\)](#), the intersection of the $\text{SU}(2)_{\text{CMB}}$ -band $r_s(z_*)$ is well contained within this $1-\sigma$ range. According to our discussion in Appendix C, however, none of these statements can be considered physical due to imprecise freeze-out conditions. Rather, we argue that, due to the finite widths of D_{drag} and D_* , baryon-velocity and photon decoupling occur at the lower values $z_{\text{lf},*}$ and $z_{\text{lf,drag}}$ indicated in Eqs. (45) and (46), respectively. Fig. 5 indicates that the intersection of the $\text{SU}(2)_{\text{CMB}}$ -band for $r_s(z_{\text{lf,drag}})$ with the $r_s - H_0$ band of [Bernal, Verde & Riess \(2016\)](#), indeed, has an impressively large overlap with the $1-\sigma$ range of the $r_s - H_0$ band determined in [Bernal, Verde & Riess \(2016\)](#). In comparing Figs. 4 and 5 or by inspecting Eq. (45), notice also that r_s at photon-decoupling redshift $z_{\text{lf},*}$ is about 8 Mpc larger than r_s at z_* .

5 SUMMARY AND OUTLOOK

In the present work we have investigated whether a $3.4-\sigma$ discrepancy [Bernal, Verde & Riess \(2016\)](#) in the value of the present Hubble parameter H_0 can be resolved under minimal assumptions concerning the high- z matter sector. This

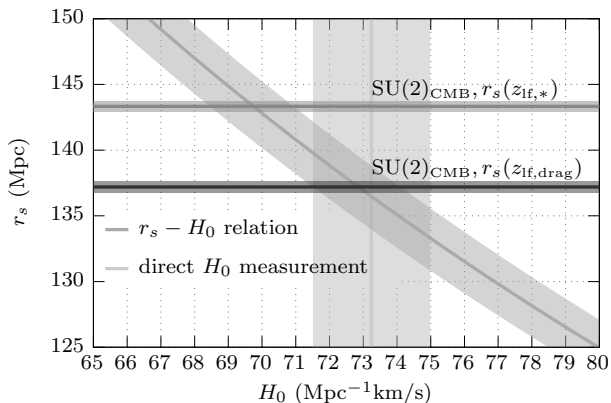


Figure 5. Prediction of the sound horizon r_s including the $1\text{-}\sigma$ error at $z_{\text{if,drag}}$ (second horizontal band) and $z_{\text{if,*}}$ (first horizontal band) in high- z $\text{SU}(2)_{\text{CMB}}$ together with the low- z r_s - H_0 relation of Bernal, Verde & Riess (2016) (curved band) and the direct measurement of H_0 (vertical band) as reported in Riess et al. (2016).

discrepancy relates to the value of H_0 as extracted by the Planck collaboration under an assumed all- z validity of the ΛCDM concordance model Ade et al. (2016) and the value directly measured in Riess et al. (2016). As suggested by our results, a new, high- z cosmology, which assumes $\text{SU}(2)_{\text{CMB}}$ thermodynamics Hofmann (2016a), solely baryonic matter, and $N_\nu = 3$ species of massless neutrinos, is a candidate. Our present analysis was enabled by a model-independent extraction of the r_s - H_0 relation (r_s the co-moving sound horizon at baryon-velocity freeze-out, observable in today’s matter correlation function) which is based on low- z observation Bernal, Verde & Riess (2016).

Interestingly, in the new model the redshift z_* , traditionally thought to set the end of hydrogen recombination, is preceded by the redshift z_{drag} proposed in Hu & Sugiyama (1996) to set the termination of the Compton drag effect. However, due to considerable widths of the visibility functions in the formal solutions of the Boltzmann hierarchy for the temperature perturbation and the Euler equation for baryon velocity we propose lower values $z_{\text{if,*}}$ and $z_{\text{if,drag}}$ than z_* and z_{drag} . Using $z_{\text{if,drag}}$ in the computation of r_s and the r_s - H_0 relation of Ref. Bernal, Verde & Riess (2016), we obtain good agreement with the directly measured value of H_0 Riess et al. (2016), see Fig. 5.

As discussed in Bernal, Verde & Riess (2016), the errors of such a direct measurement of H_0 will shrink substantially in the near future. Thus the here-proposed high- z cosmology will soon undergo increasingly stringent tests. It remains to be investigated what the influence of this model on higher acoustic harmonics and the associated damping physics is. In order to decide this, a cosmological model, which interpolates high- z $\text{SU}(2)_{\text{CMB}}$ with low- z ΛCDM , is required. Based on percolated and unpercolated topological solitons of a Planck-scale axion field Frieman et al. (1995); Giacosa et al. (2008) we make a proposal for rough features of such a model in Appendix D. A first test – predicting the angular scale θ_* of the sound horizon at photon decoupling – yields consistency. This encourages the future computation

of high- l CMB power spectra (anisotropies and polarization) to provide further tests of $\text{SU}(2)_{\text{CMB}}$. However, sophisticated routines to compute the CMB power spectra like **CMBfast** or **CAMB** owe their efficiency to a Green’s function approach which, in turn, draws on the simplicity of the equations of state of the cosmological fluids in ΛCDM . Since $\text{SU}(2)_{\text{CMB}}$ is subject to a complicated equation of state at low z it is not clear whether such a Green’s function approach is feasible at all. Rather, we would expect that an old-fashioned slice-to-slice evolution is required. Thus a quick-shot run of **CMBfast** or **CAMB** under questionable approximations is not trustworthy and hence not conclusive. Therefore, together with the pressing importance of developing an observationally sound interpolating cosmological model along the lines sketched above, a substantial revision of the simulational approach to CMB power spectra is in order. Finally, we would also like to mention here that $\text{SU}(2)_{\text{CMB}}$ has a potential to successfully address the observed large-angle anomalies of the CMB. Namely, as outlined in Hofmann (2013) and detailed in Hofmann (2016a), radiative effects in $\text{SU}(2)_{\text{CMB}}$ (transverse and longitudinal contributions to the photon polarization tensor $\Pi_{\mu\nu}$), which are important for redshifts $0 \leq z \leq 2$, induce a systematic departure from statistical isotropy. This is reflected by the build-up of a cosmologically local temperature depression (due to the transverse part of $\Pi_{\mu\nu}$), defining a gradient to its slope. The associated mild breaking of isotropy in the CMB temperature map would influence the low lying CMB multipoles and create intergalactic magnetic fields (due to the longitudinal part of $\Pi_{\mu\nu}$).

ACKNOWLEDGEMENTS

We would like to thank Jose Luis Bernal and Adam Riess for providing us with their data files on the low- z r_s - H_0 relation and the direct measurement of H_0 , and we would like to acknowledge the induction of a rewarding revision process by a very constructive and competent Reviewer. Moreover, we thank the Centre National de la Recherche Scientifique (CNRS) for the funding of RH during a one-month stay at INLN (Nice) where, among other projects, this work was conceived. Finally, RH would like to thank Thierry Grandou of INLN for his hospitality and very useful conversations.

REFERENCES

- Abazajian K. et al., 2003, *AJ*, 126, 2081
- Ade P. A. R. et al., 2014, *A&A*, 571, A1
- Ade P. A. R. et al., 2014, *A&A*, 571, A16 [arXiv:1303.5076v3]
- Ade P. A. R. et al., 2016, *A&A*, 594, A13 [arXiv:1502.01589]
- Adelman-McCarthy J. K. et al., 2008, *ApJS*, 175, 297
- Adler S. L., 1969, *Phys. Rev.*, 177, 2426
- Adler S. L., Bardeen W. A., 1969, *Phys. Rev.*, 182, 1517
- Bell J. S., Jackiw R., 1969, *Nuovo Cim. A*, 60, 47
- Beringer J. et al., 2012, *Phys. Rev. D*, 86, 010001
- Bernal J.-L., Verde L., Riess A. G., 2016, *JCAP*, 10, 019 [arXiv:1607.05617]
- Bond J.R., Efstathiou, G.. 1984, *ApJ*, 285, L45
- Fixsen D. J. et al., 1996, *ApJ*, 473, 576
- Frieman J. A., Hill C. T., Stebbins A., Waga I., *Phys. Rev. Lett.*, 75, 2077
- Fujikawa K., 1979, *Phys. Rev. Lett.*, 42, 1195

- Fujikawa K., 1980, Phys. Rev. D, 21, 2848, Erratum-ibid, 1980, Phys. Rev. D, 22, 1499
- Harrington B. J, Shepard H. K., 1977, Phys. Rev. D, 17, 2122
- Hinshaw G. F. et. al., 2013, ApJ 208, 19H
- Hofmann R., 2013, Nature Phys., 9, 686
- Hofmann R., 2015, Annalen d. Physik, 527, 254
- Hofmann R., 2016, The Thermodynamics of Quantum Yang-Mills Theory: Theory and Applications. second edition, World Scientific Publishing Co. Pte. Ltd., Singapore
- Hofmann, R., 2016, Entropy, 18(9), 310 [arXiv:1604.05136]
- Hu W., Sugiyama N., 1996, ApJ, 444, 489 [arXiv:astro-ph/9407093]
- Hu W., Sugiyama N., 1996, ApJ, 471, 542 [arXiv:astro-ph/9510117]
- Kraan T. C., van Baal P., 1998, Phys. Lett. B, 428, 268
- Kraan T. C., van Baal P., 1998, Nucl. Phys. B, 533, 627
- Lee K., Lu C., 1998, Phys. Rev. D, 58, 025011-1
- Luzzi, G. et. al., 2015, JCAP, 09, 011 [arXiv:1502.07858]
- Mather J. C. et al., 1990, ApJ, 354, L37
- Mukhanov V., 2005, Physical Foundations of Cosmology, Cambridge University Press, New York
- Muller, S. et al., 2013, A&A, 551, A109 [arXiv:1212.5456]
- Nahm W., 1980, Phys. Lett. B, 90, 413
- Nahm W., 1981, CERN preprint TH-3172
- Nahm W., 1982, in Craigie N., ed., Monopoles in Quantum Field Theory, World Scientific, Singapore, p. 87
- Nahm W., 1983, in Trieste Group Theor. Method, p. 189
- Giacosa F. et al., 2008, JHEP, 0802, 077 [arXiv:0801.0197v2]
- Peebles P.J.E., Wilkinson D.T., 1968, Phys. Rev., 174, 2168
- Peccei R. D., Quinn H. R., 1977, Phys. Rev. D, 16, 1791
- Peccei R. D., Quinn H. R., 1977, Phys. Rev. D, 38, 1440
- Perlmutter S. et al., 1998, ApJ, 517, 565
- Rephaeli, Y., 1980, ApJ, 241, 858.
- Riess A. et al., 1998, AJ, 116, 1009
- Riess A. G. et al., 2016, ApJ, 826, 56 [arXiv:1604.01424]
- Scott D., Moss A., 2009, MNRAS, 397, 445 [arXiv:0902.3438]
- Seager S., Sasselov D., Scott D., 1999, ApJ, 523, L1
- Seager S., Sasselov D., Scott D., 2000, ApJS, 128, 407
- Wetterich C., 2001, Phys. Lett. B, 522, 5
- Wong W. Y., Moss A., Scott D., 2008, MNRAS, 386, 1023 [arXiv:0711.1357]
- website: <http://www.astro.ubc.ca/people/scott/recfast.html> (accessed: November 17, 2016)

APPENDIX A: CODE ADJUSTMENTS IN RECFAST

In Appendix A we exhibit the modifications of code `recfast` due to $SU(2)_{\text{CMB}}$.

Table A1: Differences in `recfast` code of [website \(2016\)](#) for ΛCDM versus $SU(2)_{\text{CMB}}$. For a given code line (first column) the first (second) line in second column corresponds to ΛCDM ($SU(2)_{\text{CMB}}$).

line	recfast
356	<code>fnu = (21.d0/8.d0)*(4.d0/11.d0)**(4.d0/3.d0)</code> <code>fnu = (21.d0/8.d0)*(16.d0/23.d0)**(4.d0/3.d0)</code>
358	<code>z_eq = (3.d0*(H0*C)**2/(8.d0*Pi*G*a*(1.d0+fnu)*Tnow**4))*OmegaT</code> <code>z_eq = (3.d0*(H0*C)**2/(8.d0*Pi*G*a*(4.0d0+fnu)*(Tnow*0.63d0)**4))*OmegaT</code>
421	<code>y(3) = Tnow*(1.d0+z)</code> <code>y(3) = Tnow*(1.d0+z)*0.63d0</code>
462	<code>if (zend.gt.8000.d0) then</code> <code>if (zend.gt.13000.d0) then</code>
469	<code>y(3) = Tnow*(1.d0+z)</code> <code>y(3) = Tnow*(1.d0+z)*0.63d0</code>
471	<code>else if(z.gt.5000.d0)then</code> <code>else if(z.gt.8000.d0)then</code>
475	<code>rhs = dexp(1.5d0 * dLog(CR*Tnow/(1.d0+z))</code> <code>rhs = dexp(1.5d0 * dLog(CR*Tnow*0.63d0/(1.d0+z))</code>
476	<code>- CB1_He2/(Tnow*(1.d0+z))) / Nnow</code> <code>- CB1_He2/(Tnow*(1.d0+z)*0.63d0)) / Nnow</code>
482	<code>y(3) = Tnow*(1.d0+z)</code> <code>y(3) = Tnow*(1.d0+z)*0.63d0</code>
484	<code>else if(z.gt.3500.d0)then</code> <code>else if(z.gt.5650.d0)then</code>
491	<code>y(3) = Tnow*(1.d0+z)</code> <code>y(3) = Tnow*(1.d0+z)*0.63d0</code>
496	<code>rhs = dexp(1.5d0 * dLog(CR*Tnow/(1.d0+z))</code> <code>rhs = dexp(1.5d0 * dLog(CR*Tnow*0.63d0/(1.d0+z))</code>
497	<code>- CB1_He1/(Tnow*(1.d0+z))) / Nnow</code> <code>- CB1_He1/(Tnow*0.63d0*(1.d0+z))) / Nnow</code>
505	<code>y(3) = Tnow*(1.d0+z)</code> <code>y(3) = Tnow*(1.d0+z)*0.63d0</code>
509	<code>rhs = dexp(1.5d0 * dLog(CR*Tnow/(1.d0+z))</code> <code>rhs = dexp(1.5d0 * dLog(CR*Tnow*0.63d0/(1.d0+z))</code>
510	<code>- CB1/(Tnow*(1.d0+z))) / Nnow</code> <code>- CB1/(Tnow*0.63d0*(1.d0+z))) / Nnow</code>
525	<code>Trad = Tnow * (1.d0+zend)</code> <code>Trad = Tnow * (1.d0+zend)*0.63d0</code>
560	<code>if(z.gt.8000.d0)then</code> <code>if(z.gt.13000.d0)then</code>
566	<code>else if(z.gt.3500.d0)then</code> <code>else if(z.gt.5650.d0)then</code>
570	<code>rhs = dexp(1.5d0 * dLog(CR*Tnow/(1.d0+z))</code> <code>rhs = dexp(1.5d0 * dLog(CR*Tnow*0.63d0/(1.d0+z))</code>
571	<code>- CB1_He2/(Tnow*(1.d0+z))) / Nnow</code> <code>- CB1_He2/(Tnow*0.63d0*(1.d0+z))) / Nnow</code>
576	<code>else if(z.gt.2000.d0)then</code> <code>else if(z.gt.3200.d0)then</code>
579	<code>rhs = dexp(1.5d0 * dLog(CR*Tnow/(1.d0+z))</code> <code>rhs = dexp(1.5d0 * dLog(CR*Tnow*0.63d0/(1.d0+z))</code>
580	<code>- CB1_He1/(Tnow*(1.d0+z))) / Nnow</code> <code>- CB1_He1/(Tnow*0.63d0*(1.d0+z))) / Nnow</code>
589	<code>rhs = dexp(1.5d0 * dLog(CR*Tnow/(1.d0+z))</code> <code>rhs = dexp(1.5d0 * dLog(CR*Tnow*0.63d0/(1.d0+z))</code>
590	<code>- CB1/(Tnow*(1.d0+z))) / Nnow</code> <code>- CB1/(Tnow*0.63d0*(1.d0+z))) / Nnow</code>
660	<code>Trad = Tnow * (1.d0+z)</code>

Continued on next page

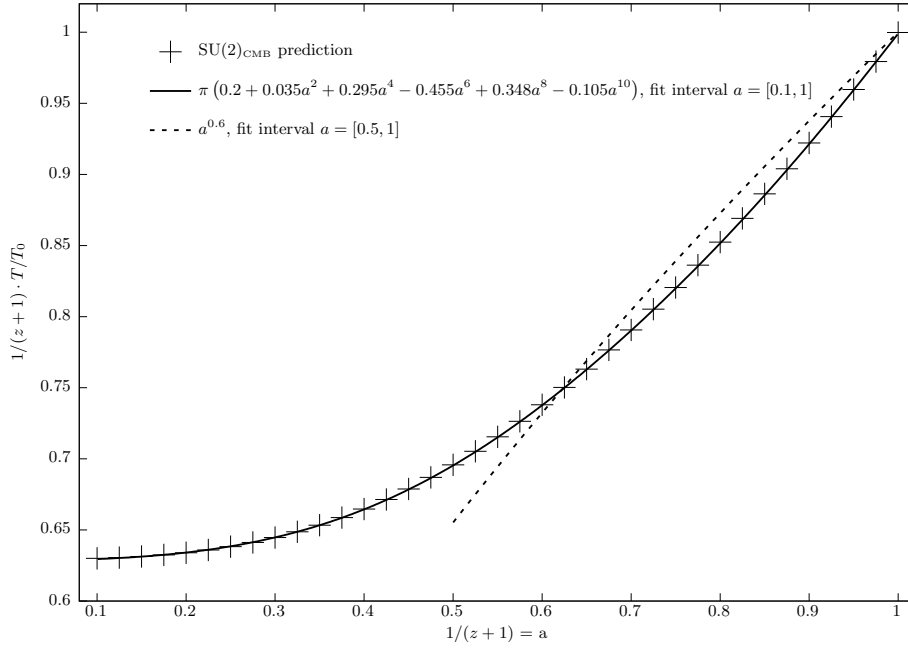


Figure B1. Low- z behaviour of function $\frac{1}{z+1} \frac{T}{T_0}$ for $SU(2)_{\text{CMB}}$. Crosses denote the prediction from $SU(2)_{\text{CMB}}$, the solid line represents the best fit to an even-power polynomial of degree ten in $\frac{1}{z+1}$ for $0 \leq z \leq 9$, and the dashed line shows the best fit to the power law $(z+1)^{-\beta}$ for $0 \leq z \leq 1$ ($\beta = 0.6$).

Table A1 – continued from previous page

line	recfast
	$\text{Trad} = \text{Tnow} * 0.63\text{d}0 * (1.\text{d}0 + z)$
805	$f(3) = \text{Tnow}$
	$f(3) = \text{Tnow} * 0.63\text{d}0$

APPENDIX B: FIT OF THE LOW- Z BEHAVIOUR OF $T(Z)$ IN $SU(2)_{\text{CMB}}$

In Appendix B we show that $T(z)$, obtained by solving the equation for energy conservation of $SU(2)_{\text{CMB}}$ in an FLRW universe Hofmann (2015) (with a slight and inessential correction of the high- z coefficient from 0.62 to 0.63), cannot be well fitted to the power law $T(z)/T_0 = (1+z)^{1-\beta}$ (β constant) assumed in "extractions" of $T(z)$ from the thermal Sunyaev-Zel'dovich effect for $0 \leq z \leq 1$, see, e.g. Luzzi et al. (2015). This is demonstrated in Fig. B1

APPENDIX C: BARYON VELOCITY DECOUPLING

Appendix C provides arguments why the commonly used criterion involving the drag depth τ_{drag} , as introduced in Hu & Sugiyama (1996) to characterise the freeze-out of baryon velocity v_b during recombination, is imprecise. Namely, we show that condition $\tau_{\text{drag}} = 1$ essentially determines the maximum $z_{\text{max,drag}}$ of a localized, yet finite-width distribution $D_{\text{drag}}(z', z)$ (with variable z' and, essentially, independence of z) during recombination. It is the z' -integral over $D_{\text{drag}}(z', z)$ down to z which determines the freeze-out behaviour of v_b in z . Here freeze-out of v_b means $v_b \propto a^{-1}$. Thus $v_b a$ can be considered constant in z only if the z' -integration starts to include the left flank (lf) of $D_{\text{drag}}(z', z)$, that is for $z \leq z_{\text{lf,drag}}$. For a (positive) bump-like distribution the left-flank position $z_{\text{lf,drag}}$ coincides with the position $z_{\text{max,drag}}$ of the maximum of $\frac{dD_{\text{drag}}}{dz'}$. As we shall show below, $z_{\text{lf,drag}}$ is considerably lower than $z_{\text{max,drag}}$ for both $SU(2)_{\text{CMB}}$ and ΛCDM .

The decoupling of the CMB photons and baryon velocity at co-moving wave number k (omitted as a subscript in the following) during recombination is described by a Boltzmann hierarchy for the temperature perturbation Θ_l Bond & Efstathiou (1984)⁵, the Einstein-Poisson equations for the metric and Newtonian gravitational potential, Φ and Ψ , respectively, and the

⁵ By virtue of Peebles & Wilkinson (1968) Θ_1 can be interpreted as the velocity of the photon fluid.

continuity and Euler equations for the coupled baryon-photon fluid [Hu & Sugiyama \(1995\)](#). Only the Euler equation is needed for the following argument. It reads [Hu & Sugiyama \(1995\)](#)

$$\dot{v}_b = -\frac{\dot{a}}{a}v_b + k\Psi + \dot{\tau}_{\text{drag}}(\Theta_1 - v_b), \quad (\text{C1})$$

where overdots represent derivatives w.r.t. conformal time, $\eta = \int_0^t \frac{dt'}{a(t')}$, $\dot{\tau}_{\text{drag}} \equiv \frac{\dot{\tau}}{R}$ with $\dot{\tau} \equiv \chi_e n_e^b \sigma_T a$ and R, n_e^b, χ_e defined in Eqs. (16), (33), (34), respectively. As usual, σ_T denotes the Thomson cross section. Varying the coefficient K in the solution

$$av_b = K e^{-\int_0^\eta d\eta' \dot{\tau}_{\text{drag}}(\eta')} \equiv K e^{-\tau_{\text{drag}}(\eta)} \quad (\text{C2})$$

of the homogeneous part

$$\dot{v}_b = -\frac{\dot{a}}{a}v_b - \dot{\tau}_{\text{drag}}v_b \quad (\text{C3})$$

of Eq. (C1), we obtain the following solution to the full equation (C1)

$$av_b(\eta) = \lim_{\epsilon \searrow 0} \int_\epsilon^\eta d\eta' e^{-\tau_{\text{drag}}(\eta', \eta)} a(\eta') (\dot{\tau}_{\text{drag}}(\eta')\Theta_1(\eta') + k\Psi(\eta')), \quad (\text{C4})$$

where $\tau_{\text{drag}}(\eta', \eta) \equiv \int_{\eta'}^\eta d\eta'' \dot{\tau}_{\text{drag}}(\eta'')$, and av_b is subject to the (Big-Bang) initial condition $a(0) = 0$. Ignoring the effect of the gravitational potential⁶ Ψ , the authors of [Hu & Sugiyama \(1996\)](#) argue that, independently of η , the factor

$$F_{\text{drag}}(\eta', \eta) \equiv e^{-\tau_{\text{drag}}(\eta', \eta)} \dot{\tau}_{\text{drag}}(\eta') \quad (\text{C5})$$

behaves like a delta function, centered at $\eta' = \eta_{\text{max}}$, which would imply that decoupling⁷ occurs for $\eta \geq \eta_{\text{max}}$. This, however, is imprecise since F_{drag} has a finite width. Namely, re-writing the solution (C4) in terms of redshift z , we have

$$\begin{aligned} av_b(z) &= \lim_{Z \nearrow \infty} \int_z^Z dz' \frac{e^{-\tau_{\text{drag}}(z', z)}}{H(z')(z'+1)} (\dot{\tau}_{\text{drag}}(z')\Theta_1(z') + k\Psi(z')) \\ &\sim \lim_{Z \nearrow \infty} \int_z^Z dz' D_{\text{drag}}(z', z)\Theta_1(z'), \end{aligned} \quad (\text{C6})$$

where (with a slight abuse of notation)

$$\tau_{\text{drag}}(z', z) \equiv \int_z^{z'} dz'' \frac{\dot{\tau}_{\text{drag}}(z'')}{H(z'')}. \quad (\text{C7})$$

In Eq. (C6) we have defined

$$D_{\text{drag}}(z', z) \equiv \frac{e^{-\tau_{\text{drag}}(z', z)} \dot{\tau}_{\text{drag}}(z')}{H(z')(z'+1)}, \quad (\text{C8})$$

and, for the reason given above, the gravitational potential Ψ was ignored in going from the first to the second line. Fig. C1 indicates D_{drag} as a function of z' (z -independence) for $\text{SU}(2)_{\text{CMB}}$ and ΛCDM . Notice the closeness of z_{drag} and $z_{\text{max,drag}}$ in both models. In contrast, $z_{\text{if,drag}}$ turns out to be considerably lower. It is worth mentioning that condition (41), again, essentially describes the position of the maximum $z_{\text{max,*}}$ of the according function $D_*(z', z)$ appearing in the formal, approximate solution of the Boltzmann hierarchy for the temperature perturbation [Hu & Sugiyama \(1996\)](#), $z_* \sim z_{\text{max,*}}$. Also here $D_*(z', z)$ is broad, and one should use $z_{\text{if,*}}$ instead of z_* as a more realistic redshift for photon decoupling, see Fig. C2.

APPENDIX D: (DE-)PERCOLATING PLANCK-SCALE AXIONIC SOLITONS AND INTERPOLATION OF HIGH- Z WITH LOW- Z COSMOLOGY

Appendix D proposes a cosmological model to interpolate low- z ΛCDM with high- z $\text{SU}(2)_{\text{CMB}}$. The basic idea invokes the fact that a Planck-scale axion field φ (a pseudo Nambu-Goldstone field of dynamical chiral symmetry breaking [Adler \(1969\)](#); [Adler & Bardeen \(1969\)](#); [Bell & Jackiw \(1969\)](#); [Fujikawa \(1979, 1980\)](#) near the Planck scale [Giacosa et al. \(2008\)](#)) due to non-thermal phase transitions of the Hagedorn type in the early universe forms $\text{U}(1)$ topological solitons (vortices) subject to a size (and mass) distribution characterised by several distinct peaks. Since $\text{SU}(2)_{\text{CMB}}$ is the only deconfining-phase Yang-Mills theory up to temperatures reaching far beyond recombination, φ 's potential is given as [Peccei & Quinn \(1977a,b\)](#)

$$V(\varphi) = (\kappa\Lambda_{\text{CMB}})^4 \cdot (1 - \cos(\varphi/m_{\text{P}})) , \quad (\text{D1})$$

⁶ Since there is no cold dark matter in $\text{SU}(2)_{\text{CMB}}$ potential wells become important only long after recombination when the dark-matter component of the late-time ΛCDM model is present, see Appendix D.

⁷ Since we here consider co-moving distances on the scale of the sound horizon only it is justified to assume that Θ_1 is a slowly varying function.

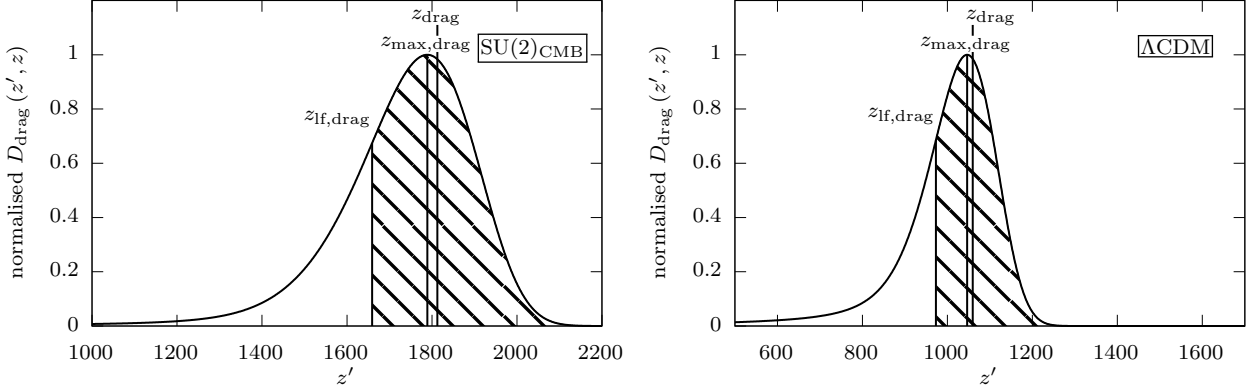


Figure C1. Normalised function $D_{\text{drag}}(z', z)$, defined in Eq. (C8), if $z \leq z_{\text{max,drag}}$ for $SU(2)_{\text{CMB}}$ (left) and ΛCDM (right). Redshift $z_{\text{lf,drag}}$ is defined as the position of the maximum of $\frac{dD_{\text{drag}}}{dz'}$ (position of left flank of D_{drag}) whereas $z_{\text{max,drag}}$ denotes the position of the maximum of D_{drag} . The value of z_{drag} , defined in Eq. (43), essentially coincides with $z_{\text{max,drag}}$: $z_{\text{drag}} = 1813 \sim z_{\text{max,drag}} = 1789$ for $SU(2)_{\text{CMB}}$ and $z_{\text{drag}} = 1059 \sim z_{\text{max,drag}} = 1046$ for ΛCDM . This should be contrasted with $z_{\text{lf,drag}} = 1659$ for $SU(2)_{\text{CMB}}$ and $z_{\text{lf,drag}} = 973$ for ΛCDM . The hatched area under the curve determines the freeze-out value of av_b .

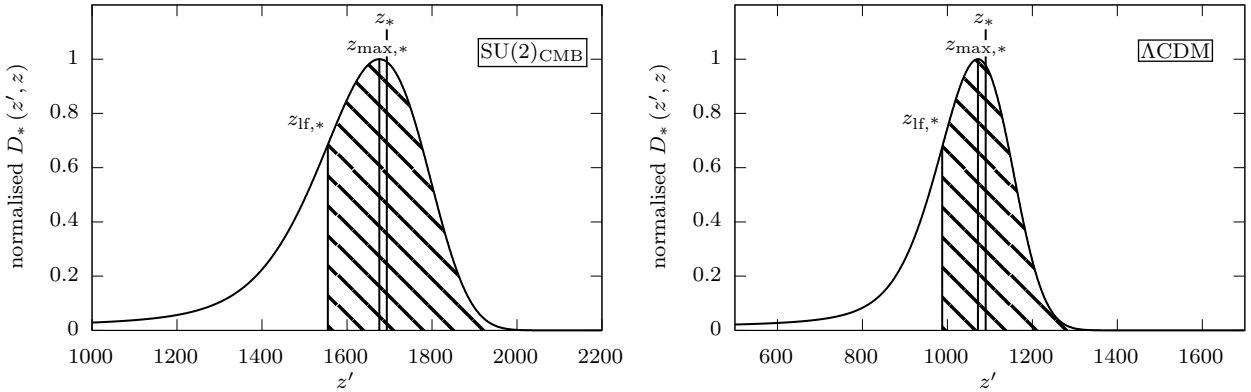


Figure C2. Normalised function $D_*(z', z)$ in analogy to Eq. (C8) but now for photon decoupling, if $z \leq z_{\text{max,*}}$ for $SU(2)_{\text{CMB}}$ (left) and ΛCDM (right). Redshift $z_{\text{lf,*}}$ is defined as the position of the maximum of $\frac{dD_*}{dz'}$ (position of left flank of D_*) whereas $z_{\text{max,*}}$ denotes the position of the maximum of D_* . The value of z_* , defined in Eq. (41), essentially coincides with $z_{\text{max,*}}$: $z_* = 1694 \sim z_{\text{max,*}} = 1676$ for $SU(2)_{\text{CMB}}$ and $z_* = 1090 \sim z_{\text{max,*}} = 1072$ for ΛCDM . This should be contrasted with $z_{\text{lf,*}} = 1555$ for $SU(2)_{\text{CMB}}$ and $z_{\text{lf,*}} = 988$ for ΛCDM . The hatched area under the curve determines the freeze-out value of the temperature perturbation.

where $\Lambda_{\text{CMB}} \sim 10^{-4}$ eV, κ is a dimensionless factor of order unity, the reduced Planck mass reads

$$m_{\text{P}} \equiv \frac{1.22 \times 10^{19}}{\sqrt{8\pi}} \text{ GeV} = (8\pi G)^{-1/2}, \quad (\text{D2})$$

and G denotes Newton's constant. Complemented by a canonical kinetic term and assuming minimal coupling to gravity, Eq. (D1) is the basis for the derivation of the according field equations to describe the self-gravitating vortex-like solitons.

Increasing z , the density of such solitons within a given, highly populated narrow size-band reaches a critical value at z_p where percolation into homogeneous and time-independent energy density occurs. (We assume instantaneous percolation). Assuming that only one such percolation point z_p occurs within $z = 0$ and $z_{p'} \gg z_{\text{lf,*}}$, we have

$$H^2 = \frac{8\pi G}{3} (\rho_b + \rho_{\text{DS}} + \rho_r) \equiv \frac{8\pi G}{3} \rho_c. \quad (\text{D3})$$

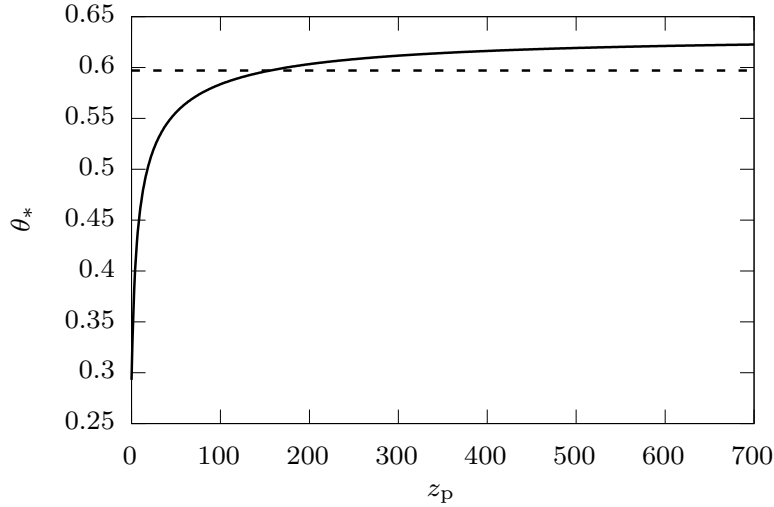


Figure D1. Function $\theta_*(z_p)$ for $\Omega_\Lambda = 0.7$, $\Omega_{\text{DM},0} = 0.26$, $\Omega_{b,0} = 0.04$, $\Omega_{\gamma,0} = 4.6 \times 10^{-5}$, and $H_0 = 73.24 \text{ km s}^{-1} \text{ Mpc}^{-1}$ for the high- z $\text{SU}(2)_{\text{CMB}}$ and low- z ΛCDM interpolating cosmological model considered in this Appendix. Also indicated is the value $\theta_* = 0.59^\circ$ (dashed line), fitted to the CMB TT power spectrum.

Here ρ_r denotes radiation-like energy density including $\text{SU}(2)_{\text{CMB}}$ and three flavours of massless neutrinos⁸. In Eq. (D3) we may approximate ρ_r as

$$\rho_r = \Omega_{\gamma,0} \rho_{c,0} \cdot \begin{cases} 0 & (z < 9) \\ A \left(1 + \frac{7}{32} \left(\frac{16}{23}\right)^{4/3} N_\nu\right) (z+1)^4 & (z \geq 9) \end{cases}, \quad (\text{D4})$$

with $A = 4(0.63)^3$, $N_\nu = 3$, and $\Omega_{\gamma,0} = 4.6 \times 10^{-5}$, compare with Eq. (24). Furthermore, $\rho_b = \Omega_{b,0} \rho_{c,0} (z+1)^3$ is the energy density of baryons. We set $\Omega_{b,0} = 0.04$. Finally, ρ_{DS} represents the dark-sector energy density, representing free vortices (dark matter) or percolated vortices (dark energy), given as

$$\rho_{\text{DS}} = \Omega_\Lambda \rho_{c,0} + \Omega_{\text{DM},0} \rho_{c,0} \cdot \begin{cases} (z+1)^3 & (z < z_p) \\ (z_p+1)^3 & (z \geq z_p) \end{cases}, \quad (\text{D5})$$

where $\Omega_{\text{DM},0} \rho_{c,0}$ is today's pressureless dark-sector energy density, represented by a gas of Planck-scale-axion vortices, and $\Omega_\Lambda \rho_{c,0}$ denotes constant vacuum energy associated with yet percolated Planck-scale-axion vortices. We set $\rho_{c,0} = \frac{3}{8\pi G} H_0^2$ with $H_0 = 73.24 \text{ km s}^{-1} \text{ Mpc}^{-1}$ Riess et al. (2016), and we use $\Omega_{\text{DM},0} = 0.26$ and $\Omega_\Lambda = 0.7$.

The observable angular scale θ_* of the sound horizon r_s at the redshift $z_{\text{If},*}$ of CMB photon decoupling is given as

$$\theta_* = \frac{r_s(z_{\text{If},*})}{\int_0^{z_{\text{If},*}} \frac{dz}{H(z)}}. \quad (\text{D6})$$

To match $\theta_* = 0.597^\circ$ fitted in Ade et al. (2016) we require $z_p = 155.4$. This yields a percentage of vacuum energy at CMB photon decoupling of about

$$\frac{\Omega_{\text{DM},0}}{\Omega_{b,0}} \left(\frac{z_p + 1}{z_{\text{If},*} + 1} \right)^3 \sim 0.65\%. \quad (\text{D7})$$

The omission of vacuum energy in our $\text{SU}(2)_{\text{CMB}}$ high- z cosmological model of Eq. (24) thus is justified for the interpolating model proposed in Appendix D.

This paper has been typeset from a $\text{T}_\text{E}\text{X}/\text{L}^\text{A}\text{T}_\text{E}\text{X}$ file prepared by the author.

⁸ For $z \leq 9$ radiation energy density is severely suppressed in the cosmological model, for $z > 9$ the thermal ground state and the masses of the vector modes of $\text{SU}(2)_{\text{CMB}}$ can be neglected.